Oxidation-Sensitive Supramolecular Polymer Nanocylinders

Clémence Nicolas, Tatiana Ghanem, David Canevet, Marc Sallé, Erwan Nicol, Christelle Gautier, Frédérick Niepceron, Olivier Colombani, Eric Levillain

Oxidation-Sensitive Supramolecular Polymer Nanocylinders

Clémence Nicolas,[1,2] Tatiana Ghanem,[2] David Canevet,[2,] Marc Sallé,[2] Erwan Nicol,[1] Christelle Gautier,[2] Eric Levillain,[2] Frédérick Niepceron,[1] Olivier Colombani[1,*]*

[1] Institut des Molécules et Matériaux du Mans (IMMM), UMR 6283 CNRS Le Mans Université, Avenue Olivier Messiaen, 72085 Le Mans Cedex 9, France.

[2] Univ Angers, CNRS, MOLTECH-Anjou, SFR MATRIX, Angers F-49000, France

KEYWORDS

Supramolecular nanocylinders, Redox-responsive, Polymer, Bisurea, Tetrathiafulvalene

ABSTRACT

This study reports the synthesis and solution self-assembly of a bis(urea) derivative decorated with a poly(ethylene oxide) chain and an electroactive tetrathiafulvalene (TTF) unit, into oxidation-sensitive supramolecular nanocylinders. As evidenced by cryo-transmission electron microscopy and light scattering experiments, the preparation pathway has a strong influence on the morphology and characteristics of the self-assembled structures, proving their frozen (out-of-

equilibrium) nature. The targeted supramolecular nanocylinders could be obtained both in aqueous medium and acetonitrile. In water, TTF can be chemically oxidized to $TTF^{\bullet+}$ by Fe(III), resulting in a very moderate disassembly of the supramolecular nanocylinders. On the contrary, TTF can be oxidized up to TTF^{2+} with the same oxidant in acetonitrile, leading to an almost complete disassembly of the nanocylinders. Oxidation of TTF eventually leads to its degradation in both solvents, even in the absence of oxygen and light. This paper shows that oxidation-sensitive supramolecular nanocylinders can be prepared in acetonitrile by combining bis(urea) and TTF units to a polymer.

Introduction

The design of 1D nanoparticles by supramolecular self-assembly of small building blocks has been the subject of growing interest.[1–3] Among these self-assemblies, supramolecular polymer bottlebrushes represent an emerging and promising field of research.[4] Such supramolecular structures result from the directional self-assembly in solution of polymers into nanocylinders decorated by polymer side-chains. The latter protect the one-dimensional structures from lateral aggregation, resulting in isolated nanocylinders in solution. The anisotropic character of isolated polymer nanocylinders makes them relevant for varied applications:[4–18] drug delivery,[19,20] synthesis of mesoporous inorganic materials,[21] catalysis,[22] organic electronics,[23] or emulsion stabilization.[24] Imparting stimuli-responsiveness to supramolecular nanocylinders may allow their disassembly after use, which can be critical to reach reversibly-controlled systems. For example, a reversible destabilisation of an emulsion can be conducted in order to recover the products of a reaction.[25]

In principle stimuli-responsive polymer nanocylinders can be prepared *via* the self-assembly of amphiphilic block copolymers.[26–32] However, this approach presents several limitations. First, cylindrical micelles are thermodynamically stable in a very limited compositional window of the blocks,[29,33] making their preparation less accessible in comparison to spherical micelles.[29] Second, many amphiphilic block copolymers form out-of-equilibrium (frozen) structures in solution[34] so that cylindrical structures are not necessarily obtained even when they are thermodynamically expected.[29,30,35] Finally, with amphiphilic copolymers, morphological transitions always rely on a response of the polymer blocks to a stimulus (pH, T, light, redox...). This strategy therefore depends on the chemical nature of the polymer and lacks versatility.

An emerging alternative for the design of supramolecular nanocylinders based on polymers has recently been reviewed by Brendel and coworkers.[4] It relies on directional interactions such as π-stacking, or more frequently hydrogen bonds, which drive the formation of 1D assemblies. Strong and cooperative hydrogen bonding assembling units, such as C_3-symmetric, linear or cyclic oligopeptides, ureidopyrimidinone, squaramides and urea units are necessary to promote the formation of long nanocylinders in spite of the steric hindrance caused by the polymer chains. With this strategy, cylindrical particles can be formed irrespective of the length of the polymer chains, making this approach more versatile than using amphiphilic block copolymers.[36,37] To date, different attempts to design stimuli-responsive supramolecular polymer nanoparticles based on hydrogen bonding units have been reported.[38–49] To the best of our knowledge, all reports have been obtained with polymers bearing linear or cyclic peptides, leading to supramolecular bottlebrush polymers responsive to pH,[39,40,43,44] reduction,[42,46] oxidation,[45] temperature,[40] or host-guest interactions.[47] In most examples, the responsiveness of the supramolecular structures is due to the sensitivity of the polymer arms to stimuli: pH sensitive polymers can be charged, resulting

in repulsive interactions which disrupt the assemblies,[39,40,43] while temperature-sensitive polymers can be made hydrophobic, resulting in aggregation of nanocylinders into micrometric particles.[40] The latter examples are therefore also polymer-dependent. Only three examples rely on stimulation of the self-assembling units to prepare responsive supramolecular bottlebrushes. Otter *et al.* demonstrated that pH-sensitive supramolecular nanocylinders based on oligopeptides can be disassembled through the creation of charges within the self-assembling unit, resulting in electrostatic repulsions.[44,45] Song *et al.* developed cyclic oligopeptides decorated with two phenyl rings.[47] Complexation of the latter by cucurbituril cumbersome cages increases steric hindrance and elegantly disrupts the self-assemblies. Otter *et al.*[45] recently reported the only example of oxidation-sensitive supramolecular bottlebrushes. Here, the disruption of the nanocylinders into small spheres is triggered by enzyme-mediated oxidation of the thioether functions constituting the assembling unit.

Considering the potential of stimuli responsive supramolecular nanocylinders, we investigated another redox-responsive assembling unit consisting of a bis(urea) (U_2) moiety as a strong cooperative hydrogen bonding motif,[50] connected to a redox responsive tetrathiafulvalene (TTF) unit.[51] This choice presents several advantages compared to the system developed by Otter *et al*. First, TTF can in principle be reversibly oxidized to two different states: the radical cation $TTF^{\bullet+}$ and the dication TTF^{2+}.[52] Moreover, TTF, $TTF^{\bullet+}$ and TTF^{2+} exhibit different colors, allowing to monitor their formation by direct visual observation or UV-visible absorption spectroscopy. Finally, TTF constitutes a planar electron rich unit that readily forms charge transfer complexes with electron withdrawing moieties, which could be of interest for future studies. In particular, we recently successfully prepared homogeneous[53] and Janus[54] supramolecular bottlebrush polymers in aqueous medium using hydrophilic polymer chains decorated with a bis(urea) fragment and

either electron acceptor (naphthalene diimide) or donor (dialkoxynaphthalene) units. Replacing the latter by TTF may result into redox-responsive Janus nanocylinders which could be very efficient smart emulsion stabilizers. Finally, it has to be noted that TTF was already successfully used to design redox-responsive molecular organogelators[55–58] or isotropic polymer particles[59,60] but never in redox-responsive supramolecular bottlebrushes.

To investigate the concept, a hydrophilic poly(ethylene) oxide (PEO) polymer was therefore functionalized by the combination of a TTF and a bis(urea) unit, yielding **PEO-TTF-U$_2$** (**Scheme 1**).

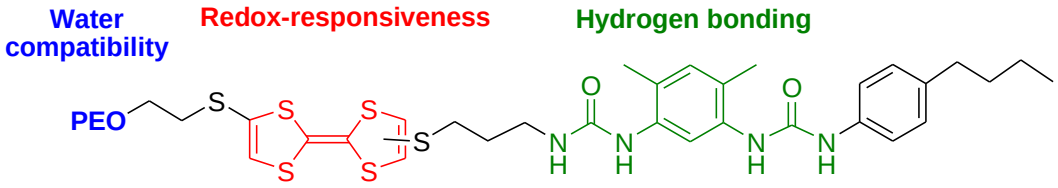

Scheme 1. Chemical structure of **PEO-TTF-U$_2$**

Results and discussion

1. Synthesis of PEO-TTF-U$_2$

The multifunctional polymer **PEO-TTF-U$_2$** was synthesized from a new TTF derivative (**1**, **Scheme 2**). The latter was obtained by the desymmetrization of the bis(2-cyanoethylsulfanyl) tetrathiafulvalene (**c**, SI, section 1.2),[61] *via* selective deprotection of a thiolate function with cesium hydroxide monohydrate (1 equiv.) in DMF and subsequent nucleophilic substitution on N-(3-bromopropyl)phthalimide (**Scheme 2**). Intermediate **1** was obtained in 44% yield after purification by silica gel chromatography. The remaining thiolate function of **1** was subsequently deprotected in order to proceed to the TTF functionalization with mesylated-PEO (**d**, SI, section 1.2, M_n = 2000 g/mol, Đ = 1.1), leading to **2**. Note that **1** was used in a 1:0.33 ratio compared to mesylated-

PEO in order to limit the amount of non-functional polymer chains. **2** was moreover purified by preparative SEC working in recycling conditions to get rid of impurities (SI, section 1.2). Hydrazinolysis of the phthalimide group of **2** was then performed, yielding the amine-terminated polymer **3**. The latter was eventually used to prepare the targeted redox-active bis(urea) polymer **PEO-TTF-U$_2$** with an overall yield of 19%, through reaction with isocyanate intermediate **4**.

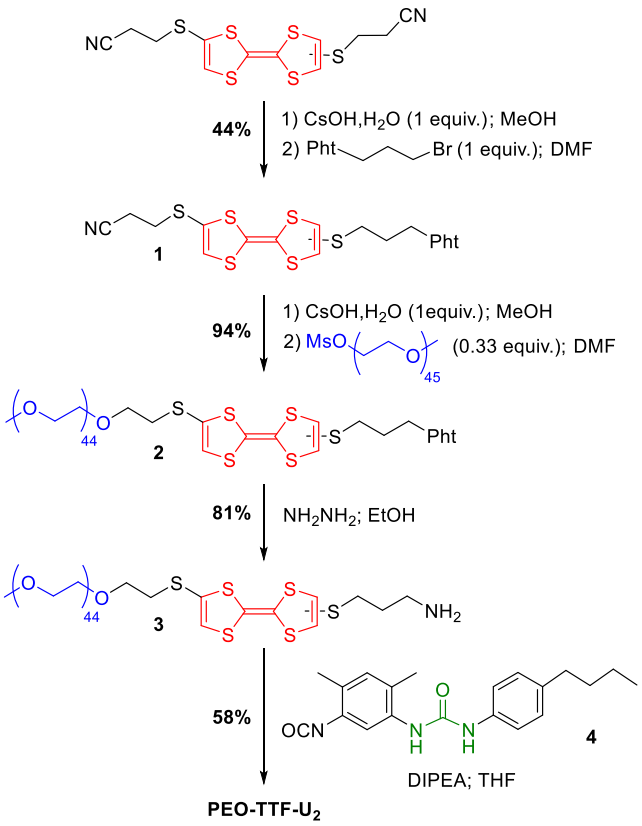

Scheme 2. Synthesis of the target polymer **PEO-TTF-U$_2$**

2. Self-assembly and oxidation sensitivity of PEO-TTF-U$_2$ in aqueous medium

The self-assembly of **PEO-TTF-U$_2$** was first investigated in aqueous medium by directly dispersing the polymer in water. The corresponding suspensions were studied by cryoTEM analysis and light scattering, which revealed the formation of small and weakly aggregated monodisperse spherical particles (R_h = 7 nm and N_{agg} = 44) instead of the targeted one-dimensional

assemblies (see SI, section 2.3.1). A second preparation pathway, deemed "DMSO-route",[24,53,54] was therefore attempted: **PEO-TTF-U$_2$** was dissolved in DMSO, a strong hydrogen bond competitor which favors its unimer state, and water was slowly added to reach a water/DMSO content of 99/1 (v/v) (see SI, section 2.2). CryoTEM experiments revealed that this method mainly leads to the formation of nanocylinders (**Figure 1a**), as well as a small amount of spheres. The nanocylinders exhibit a polydisperse length of several hundreds of nanometers and a monodisperse diameter of *ca.* 10 nm. Additional characterization by static (**Figure 2**) and dynamic light scattering experiments yielded the following characteristics for the nanocylinders: N_{agg} = 340, R_g ~ 60 nm, R_h = 24 nm. The values of R_g and R_h faithfully represent the characteristics of the nanocylinders in spite of the presence of spheres whose contribution to these parameters is negligible. The large value of R_g/R_h = 3 is consistent with the formation of anisotropic particles. The value of N_{agg} must be considered as a lower estimate of the aggregation number of the nanocylinders because of the presence of spheres (see SI section 2.3.2 for details).

The strong influence of the preparation pathway ("direct dispersion in water" *vs.* "DMSO-route") on the characteristics of the assemblies reveals that the particles formed by **PEO-TTF-U$_2$** are out-of-equilibrium (frozen) in aqueous medium. Nevertheless, according to light scattering, nanocylinders can be prepared reproducibly with the "DMSO-route" and are stable. Indeed, the characteristics of **PEO-TTF-U$_2$** nanocylinders prepared following the "DMSO route" did not evolve between 24 h and 1 month (**Figure S18**). Moreover, independent preparations yielded fairly reproducible results (**Figure S19**).

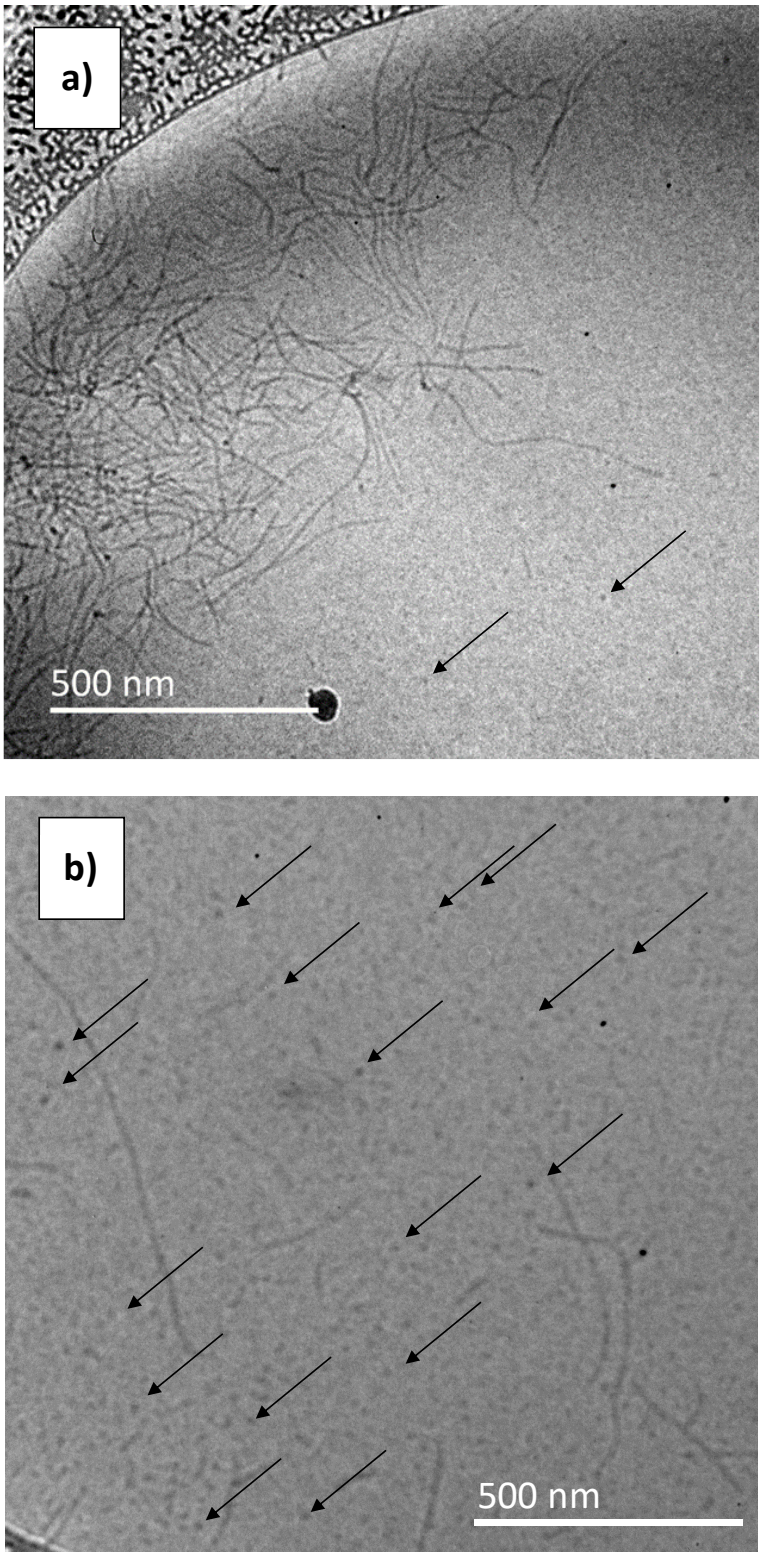

Figure 1. CryoTEM of particles formed by **PEO-TTF-U$_2$** with the "DMSO-route" (water/DMSO = 99/1 v/v, C = 1 g.L^{-1}) a) before oxidation, revealing long nanocylinders and a few nanospheres

(indicated by arrows) and b) after oxidation with Fe^{3+} (100 equiv.), showing that nanocylinders are still present but that the proportion of spheres (some of which are indicated by arrows) strongly increased. Additional pictures are shown on **Figure S21**.

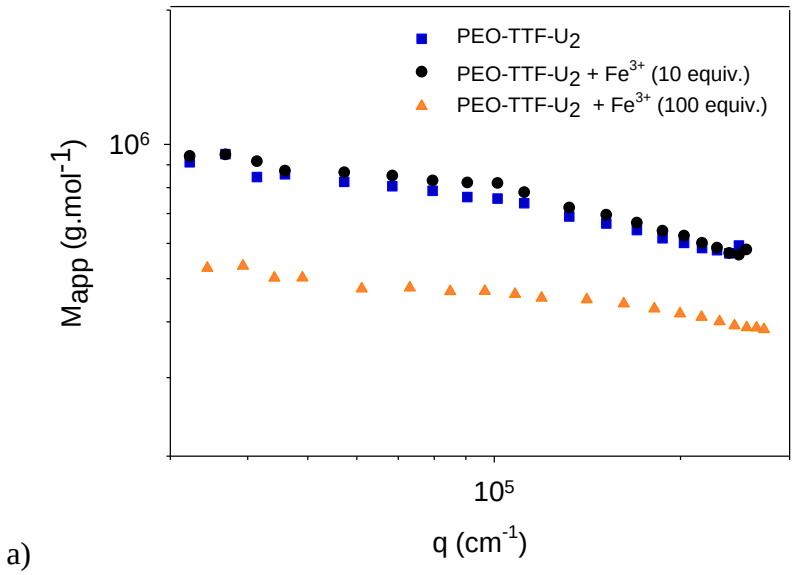

a)

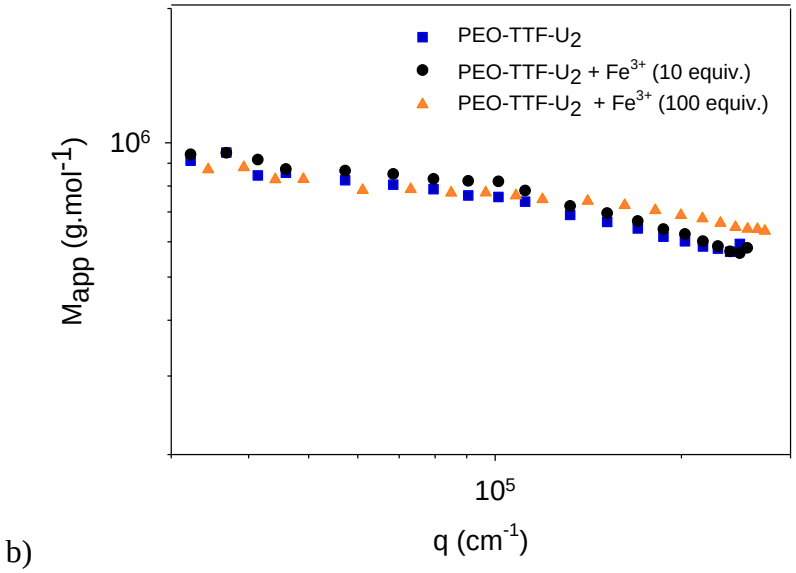

b)

Figure 2. a) Angular dependency of the apparent molar mass of **PEO-TTF-U₂** self-assemblies (0.5 $g.L^{-1}$ prepared *via* the "DMSO-route") in water/DMSO (99/1 v/v) before and after oxidation

with Fe^{3+}. b) Same data after shifting the curve corresponding to 100 eq. of Fe^{3+} vertically by a factor 1.6 to facilitate comparison.

The ability of TTF to be oxidized in $TTF^{\bullet+}$ or TTF^{2+} was exploited to trigger the disassembly of the nanocylinders. To this end, the chemical oxidation of the **PEO-TTF-U2** dispersions in water/DMSO (99/1) was performed using iron (III) perchlorate $Fe(ClO_4)_3$ and monitored by UV-visible absorption spectroscopy.[59] Many anions being known as hydrogen bond competitors,[62] we first checked that the perchlorate counter-ion ClO_4^- did not impact the self-assembly process of **PEO-TTF-U2**. Light scattering revealed no effect on the nanocylinders prepared by the "DMSO-route" (0.5 g/L) with 0.1 M $LiClO_4$, corresponding to about 400 equivalents of ClO_4^- relative to the bis(urea) units (**Figure S23**). When one equivalent of Fe^{3+} was added to the solution of **PEO-TTF-U2** in water/DMSO 99/1, the characteristic absorption bands of $TTF^{\bullet+}$ were surprisingly not observed. However, adding 10 or 100 equivalents at once led to the appearance of the characteristic absorption bands of $TTF^{\bullet+}$ (420 and 650 nm) and its corresponding radical cation dimer $(TTF^{\bullet+})_2$ (850 nm) (**Figure 3a**).[63] These absorption bands proved to gradually vanish (the absorbance at 420, 650 and 850 nm was roughly halved within 1 h and absent after 20 h, **Figure 3b).** Since Adeel *et al.* reported the photoreduction of $TTF^{\bullet+}$ in water,[64] these experiments were repeated in anaerobic and dark conditions, affording the same results. Furthermore, adding Fe^{3+} to the corresponding solutions did not allow for observing the reappearance of the typical radical cation absorption bands, confirming that the time evolution of the UV-visible absorption spectra (**Figure 3b**) is not caused by a reduction of $TTF^{\bullet+}$ back to the TTF neutral state, but by its degradation. To assess the potential role of DMSO in this singular situation, oxidation experiments were also performed with **PEO-TTF-U2** in pure water (in the dark and absence of dioxygen) and gave similar results, showing that DMSO is not responsible for the degradation of $TTF^{\bullet+}$ (**Figure S24**).

Altogether, these observations reveal the instability of this radical cation in water and show this behaviour is not related to DMSO, light and/or dioxygen. Neither the origin of this phenomenon (specific chemical structure of **PEO-TTF-U2**, self-assembly...) nor its mechanism (gradual conversion of $TTF^{\bullet+}$ into TTF^{2+} which is known to rapidly degrade in water[64] or intrinsic instability of $TTF^{\bullet+}$ in these conditions) are known. To our knowledge, such a behaviour has never been documented in the literature.

In view of these results, it seems reasonable to state that the rate of $TTF^{\bullet+}$ formation increases with the number of Fe(III) equivalents and that using only one equivalent of Fe(III), the formation of $TTF^{\bullet+}$ is slow in comparison to the rate of degradation. This may explain why $TTF^{\bullet+}$ was not detectable by UV-visible absorption spectroscopy when adding one equivalent of Fe(III). On the contrary, with 10 or 100 equivalents of Fe(III), the $TTF^{\bullet+}$ concentration appears higher, which suggests it is formed sufficiently rapidly to be observed before it degrades.

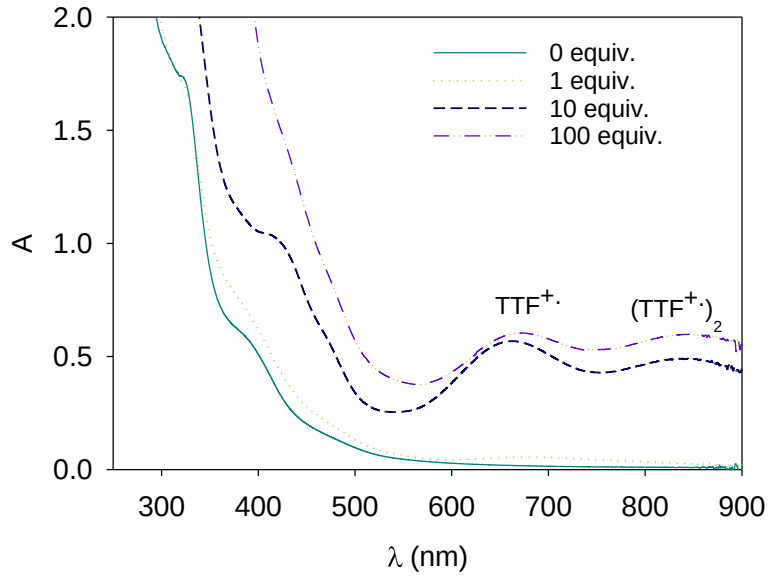

a)

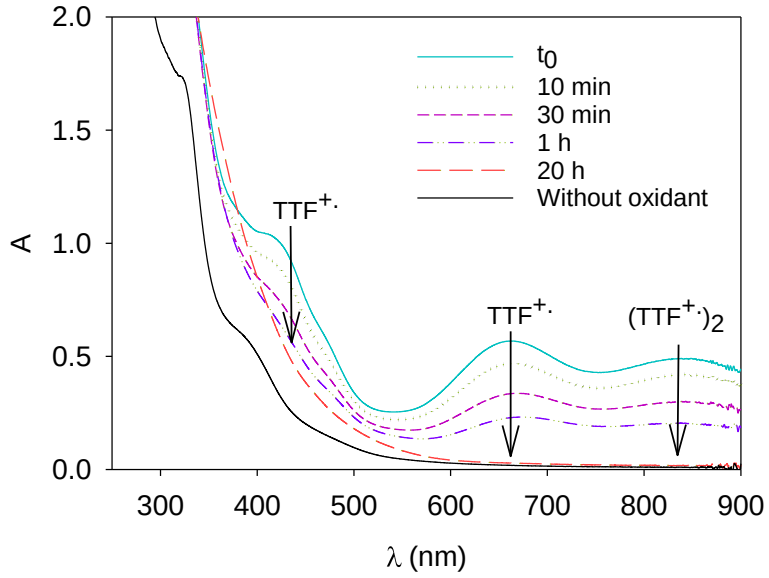

b)

Figure 3. a) UV-visible absorption spectra of **PEO-TTF-U2** dispersions (C = 0.5 g.L^{-1}) in water/DMSO (99/1) before oxidation (0 equivalent of Fe^{3+}) and right after (< 1 min) the addition of 1, 10 and 100 equivalents of Fe^{3+}. b) UV-visible absorption spectra of **PEO-TTF-U2** (0.5 g.L^{-1}) in water/DMSO (99/1) before oxidation (without oxidant) as a function of time after the addition of 10 equivalents of Fe^{3+}.

The impact of the chemical oxidation of TTF on the self-assemblies of **PEO-TTF-U2** in water/DMSO (99/1 v/v) was then investigated. No alteration of the self-assemblies was noticed by light scattering with 10 equivalents of Fe^{3+} in spite of the formation of $TTF^{\bullet+}$ (**Figure 2**). With 100 equivalents of Fe^{3+}, a decrease by a factor of 1.6 (40%) of the scattered intensity at low q was observed, indicating that the concentration and/or length of the nanocylinders slightly decreases. Further interpretation of the SLS and DLS data and additional cryoTEM experiments were necessary to conclude. First, cryoTEM analysis reveals that the proportion of spheres strongly increases in the presence of 100 eq. of Fe^{3+} (**Figure 1b**), indicating that part of the nanocylinders

have been disassembled into smaller spherical particles although many long nanocylinders are still present. Second, the relaxation function measured by DLS hardly changes before and after oxidation (**Figure S25**), implying that the dimensions of the largest particles (nanocylinders), which dominate the scattering signal, are hardly affected. Third, after shifting vertically the SLS data with 100 eq. of Fe^{3+} to facilitate comparison (**Figure 2b)**, a slight decrease of the slope of $M_{app} = f(q)$ seems to be observed with 100 eq. of Fe^{3+}, which is compatible with the presence of a larger proportion of spheres (which exhibit no angular dependency given their size) in the solution.

Overall, these data indicate that oxidation of TTF into $TTF^{\bullet+}$ using 100 eq. of Fe^{3+} does lead to the destruction of some nanocylinders into small spheres. However, most nanocylinders (60%) remain unaffected in spite of the huge amount of Fe^{3+} used. With 10 eq. of Fe^{3+}, which is already a very significant amount, the nanocylinders are not affected at all. To summarize, the **PEO-TTF-U$_2$** nanocylinders are not very sensitive to oxidation in aqueous medium. Different phenomena may explain this behaviour: 1) we expected that upon the generation of positive charges ($TTF^{+\bullet}$, TTF^{2+}) in the nanocylinders, ion pairing effects between the oxidized TTF species and anions (ClO_4^-) would lead to rearrangements of the supramolecular structures, making the latter more prone to dissociate. Such a behaviour was not observed in the case of **PEO-TTF-U$_2$**-based nanocylinders, which could notably result from attractive radical cation dimerization between electroactive $TTF^{\bullet+}$ units;[65,66] 2) the frozen (out-of-equilibrium) character of the nanocylinders in water prevents them from reorganizing whatever their redox state; 3) the degradation of oxidized species produces species that do not promote dissociation and occurs more rapidly than the time needed for the nanocylinders to disassemble.

3. Self-assembly and redox-sensitivity of PEO-TTF-U$_2$ in acetonitrile

Given the difficulties encountered in water, acetonitrile appeared as a valuable alternative, since 1) it is an organic solvent that efficiently solvates ion pairs such as $Fe(ClO_4)_3$ and does not constitute a hydrogen bond competitor (Hansen solubility parameters δ_H (CH_3CN) = 6.1 $MPa^{1/2}$; δ_H (H_2O) = 42.3 $MPa^{1/2}$)[67]; 2) polyethylene glycol derivatives generally display a good solubility in this solvent; 3) $TTF^{\bullet+}$ radical cations are relatively stable in this solvent,[68] and 4) TTF^{2+} can usually readily be obtained in this solvent contrary to water.[68] Attempts to prepare supramolecular nanocylinders either by direct dispersion of **PEO-TTF-U2** in acetonitrile or by first dissolving the polymer in DMSO and then slowly adding acetonitrile resulted in the formation of very large and ill-defined fractal aggregates (**Figure S26**). The nanocylinders successfully prepared in aqueous medium with the "DMSO-route" were therefore transferred into acetonitrile after dialysis and freeze drying (see SI, section 2.3.3.). It was verified that the particles transferred in this way had the same characteristics as those initially formed in water/DMSO (**Figure S27**), again indicating the frozen character of the particles even in ACN.

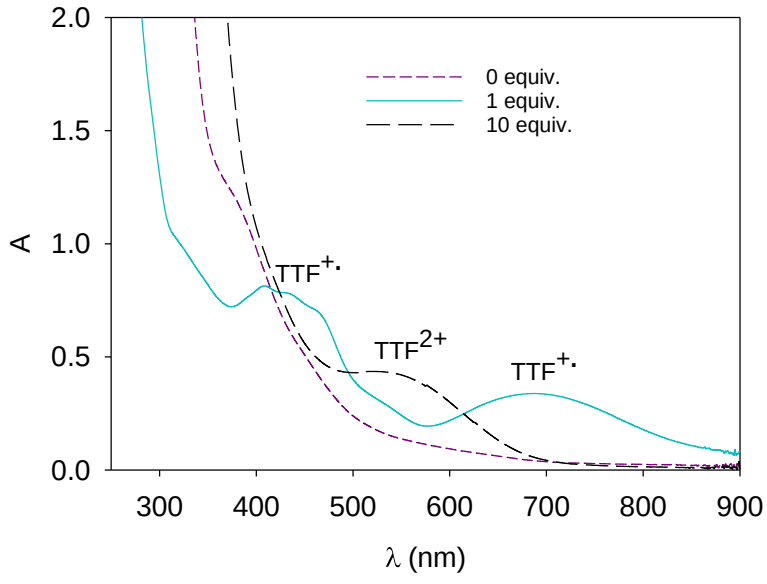

a)

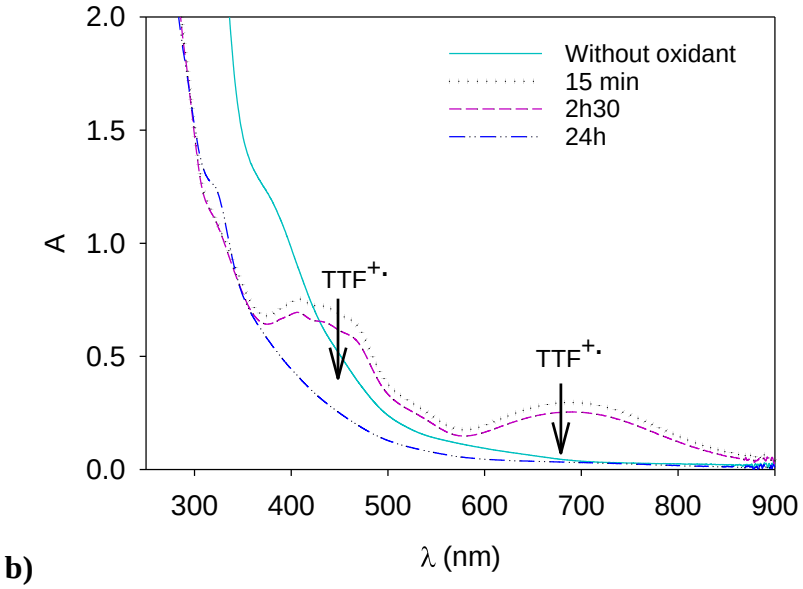

b)

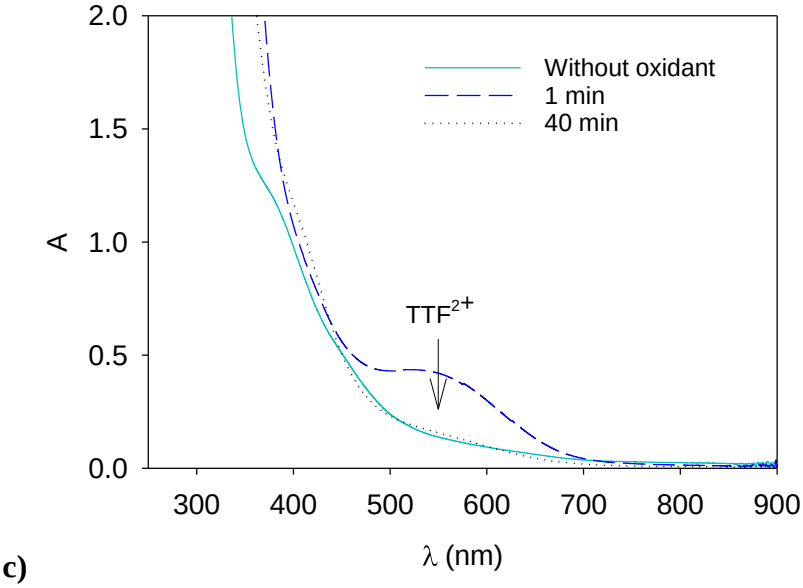

c)

Figure 4. a) UV-visible absorption spectra of **PEO-TTF-U₂** dispersions at C = 0.5 g.L^{-1} in ACN (nanocylinders transferred from the water/DMSO 99/1 v/v solution, see SI section 2.3.3.) before oxidation (0 equivalent Fe^{3+}) and right after (< 1 min) the addition of 1 or 10 equivalents of Fe^{3+}. b) UV-visible absorption spectra of **PEO-TTF-U₂** (0.5 g.L^{-1}) in ACN before oxidation (without oxidant) and for different times after the addition of 1 equivalent of Fe^{3+}. c) UV-visible absorption

spectra of **PEO-TTF-U2** (0.5 $g.L^{-1}$) in ACN before oxidation (without oxidant) and for different times after the addition of 10 equivalents of Fe^{3+}.

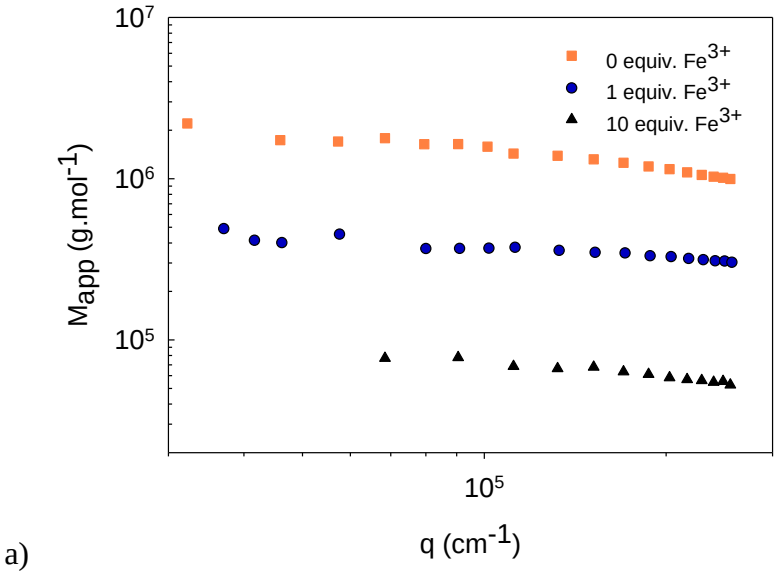

a)

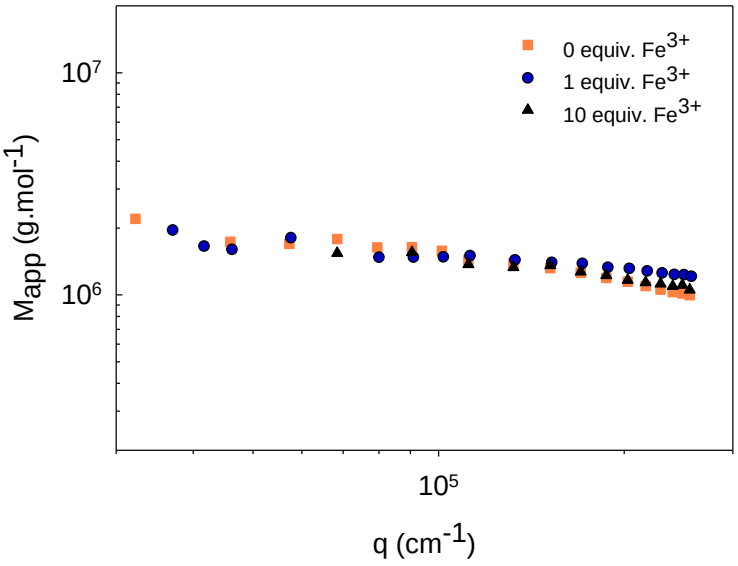

b)

Figure 5. a) Angular dependency of the apparent molar mass of **PEO-TTF-U2** dispersions at C = 0.5 $g.L^{-1}$ in ACN (nanocylinders transferred from the water/DMSO 99/1 v/v solution, see SI

section 2.3.3.) before oxidation (0 equivalent Fe^{3+}) and right after (< 1 min) the addition of 1 or 10 equivalents of Fe^{3+}. b) Same data after shifting the curves vertically by a factor 4 or 20 respectively for 1 or 10 eq. of Fe^{3+} to facilitate comparison.

The oxidation of the dispersed **PEO-TTF-U2** nanocylinders in acetonitrile was carried out with 1 or 10 equivalents of $Fe(ClO_4)_3$. With 1 equivalent of oxidant, the characteristic absorption bands of $TTF^{\bullet+}$ (450 and 700 nm) appeared (**Figure 4a**). One will also note that radical cation dimers ($\lambda_{max}(CH_3CN)$ = 780 nm)[69] were not observed and therefore, cannot contribute to the stability of the nanostructures. Degradation of $TTF^{\bullet+}$ also occurred in this solvent (even in the dark and absence of oxygen. The characteristic absorption bands of $TTF^{\bullet+}$ only slightly decreased within 2 h, but had fully disappeared after 24 h, **Figure 4b**). The corresponding samples were studied by light scattering revealing that the scattered intensity was divided by a factor 4 (**Figure 5**).

With 10 equivalents of oxidant, TTF^{2+} was formed (**Figure 4a**, $\lambda_{max}(TTF^{2+})$ = 550 nm),[69] which was not possible in water. Although this oxidized form was not stable either (it fully degraded within less than one hour, see **Figure 4c**, and the degraded species could not be reoxidized), its generation had a dramatic effect on the assemblies: the scattered intensity was divided by a factor 20, reaching 5% of its initial value (**Figure 5**). Neither the q-dependency of the scattered intensity (**Figure 5b**) nor the hydrodynamic radius (**Figure S28)** seem to be strongly affected upon oxidation with 10 eq. of Fe^{3+}, suggesting that the dimension of the largest particles hardly changes. We note that this result must be considered with care since the raw scattered intensity after oxidation with 10 eq. of Fe^{3+} was extremely low (only 10 times as much as the solvent), rendering the measurement less accurate. These results still undoubtedly imply that most of the nanocylinders (95% in weight) are disassembled into smaller aggregates upon oxidation, too small to contribute significantly to the scattered intensity, or into unimers. It seems that a few

nanocylinders with hardly affected dimensions are still present in solution. Considering that TTF^{2+} rapidly and irreversibly degrades, it was not possible to determine whether the very efficient disassembly of the supramolecular nanocylinders in the presence of 10 equivalents of Fe^{3+} was caused by the formation of TTF^{2+} and/or its degraded state. The irreversible disassembly was however triggered by oxidation since the nanocylinders are highly stable when TTF is neutral.

In water/DMSO (99/1 v/v), 10 equivalents of oxidant had absolutely no effect on the self-assemblies and adding 100 equivalents only led to a 40% decrease of the scattered intensity. In comparison, the results in acetonitrile are quite impressive. Among the hypotheses mentioned in the previous section, the frozen character of the assemblies cannot explain alone the quasi-insensitivity of **PEO-TTF-U$_2$** self-assemblies to oxidation in water/DMSO (99/1 v/v) since the self-assemblies are also frozen in ACN. Now, the formation of $TTF^{\bullet+}$ disturbs much more the self-assemblies in ACN than in water/DMSO (99/1 v/v), suggesting that the nanocylinders are less robust in the organic solvent and that solvophobic effects play a key role. Finally, it is clear that TTF^{2+} and/or its degraded form disrupt much more efficiently the assemblies, leading to an almost complete disassembly of the nanocylinders.

Conclusion

We successfully synthesized the bis(urea) derivative **PEO-TTF-U$_2$**, which combines a polyethylene oxide chain, an electroactive tetrathiafulvalene moiety and a hydrogen-bonding bis(urea) unit. Nanocylinders can be self-assembled from **PEO-TTF-U$_2$**, both in water and acetonitrile. Their oxidation-triggered dissociation was tested and proved to be weak in aqueous medium, even with 100 equivalents of oxidant. Remarkably, in acetonitrile the supramolecular nanocylinders can be almost fully disassembled (95%) upon oxidation of TTF into TTF^{2+},

providing the first example of a chemically-induced (Fe^{3+} addition) disassembly of supramolecular nanocylinders. The disassembly is not reversible because of the degradation of $TTF^{\bullet+}$ and TTF^{2+}, the latter being quite surprising in acetonitrile since those species are usually reported to be rather stable in organic solvent in the absence of oxygen and light. This intriguing last result must either originate from the supramolecular structure or from the chemical structure of the TTF and deserves deeper investigation. Eventually, this study constitutes a first step towards redox-sensitive supramolecular nanocylinders which are promising for varied applications, notably in the field of drug delivery or stimuli-responsive emulsions.

Acknowledgements

This work was supported by the Région Pays de Loire (France) and Le Mans Université in the frame of the SPEED program (Postdoctoral grant to C. Nicolas – RESUS project). The COMUE Angers-Le Mans is also acknowledged for funding the PEGASE project. Luke Harvey is thanked for helpful discussions. Alexandre Benard and "Plateforme spectrométrie de masse" at IMMM are thanked for the field desorption mass spectrometry measurements. The authors are also grateful to the SFR MATRIX for its contribution to NMR and mass spectrometry analyses.

References

(1) Yan, Y.; Lin, Y.; Qiao, Y.; Huang, J. Construction and Application of Tunable One-Dimensional Soft Supramolecular Assemblies. Soft Matter 2011, 7 (14), 6385–6398. https://doi.org/10.1039/C1SM05030C.

(2) Palmer, L. C.; Stupp, S. I. Molecular Self-Assembly into One-Dimensional Nanostructures. Acc. Chem. Res. 2008, 41 (12), 1674–1684. https://doi.org/10.1021/ar8000926.

(3) Kim, S.; Kim, J. H.; Lee, J. S.; Park, C. B. Beta-Sheet-Forming, Self-Assembled Peptide Nanomaterials towards Optical, Energy, and Healthcare Applications. Small 2015, 11 (30), 3623–3640. https://doi.org/10.1002/smll.201500169.

(4) Gruschwitz, F. V.; Klein, T.; Catrouillet, S.; Brendel, J. C. Supramolecular Polymer Bottlebrushes. Chem. Commun. 2020, 56 (38), 5079–5110. https://doi.org/10.1039/D0CC01202E.

(5) Wieczorek, S.; Dallmann, A.; Kochovski, Z.; Börner, H. G. Advancing Drug Formulation Additives toward Precision Additives with Release Mediating Peptide Interlayer. J. Am. Chem. Soc. 2016, 138 (30), 9349–9352. https://doi.org/10.1021/jacs.6b03604.

(6) Fernandez-Lopez, S.; Kim, H. S.; Choi, E. C.; Delgado, M.; Granja, J. R.; Khasanov, A.; Kraehenbuehl, K.; Long, G.; Weinberger, D. A.; Wilcoxen, K. M.; Ghadiri, M. R. Antibacterial Agents Based on the Cyclic D,L-Alpha-Peptide Architecture. Nature 2001, 412 (6845), 452–455. https://doi.org/10.1038/35086601.

(7) Horne, W. S.; Wiethoff, C. M.; Cui, C.; Wilcoxen, K. M.; Amorin, M.; Ghadiri, M. R.; Nemerow, G. R. Antiviral Cyclic d,l-α-Peptides: Targeting a General Biochemical Pathway in Virus Infections. Bioorg. Med. Chem. 2005, 13 (17), 5145–5153. https://doi.org/10.1016/j.bmc.2005.05.051.

(8) Ashkenasy, N.; Horne, W. S.; Ghadiri, M. R. Design of Self-Assembling Peptide Nanotubes with Delocalized Electronic States. Small 2006, 2 (1). https://doi.org/10.1002/smll.200500252.

(9) Brea, R. J.; Castedo, L.; Granja, J. R.; Herranz, M. Á.; Sánchez, L.; Martín, N.; Seitz, W.; Guldi, D. M. Electron Transfer in Me-Blocked Heterodimeric α,γ-Peptide Nanotubular Donor–Acceptor Hybrids. Proc. Natl. Acad. Sci. 2007, 104 (13), 5291–5294. https://doi.org/10.1073/pnas.0609506104.

(10) Reiriz, C.; Brea, R. J.; Arranz, R.; Carrascosa, J. L.; Garibotti, A.; Manning, B.; Valpuesta, J. M.; Eritja, R.; Castedo, L.; Granja, J. R. α,γ-Peptide Nanotube Templating of One-Dimensional Parallel Fullerene Arrangements. J. Am. Chem. Soc. 2009, 131 (32), 11335–11337. https://doi.org/10.1021/ja904548q.

(11) Motesharei, K.; Ghadiri, M. R. Diffusion-Limited Size-Selective Ion Sensing Based on SAM-Supported Peptide Nanotubes. J. Am. Chem. Soc. 1997, 119 (46), 11306–11312. https://doi.org/10.1021/ja9727171.

(12) Rodríguez-Vázquez, N.; Amorín, M.; Alfonso, I.; Granja, J. R. Anion Recognition and Induced Self-Assembly of an α,γ-Cyclic Peptide To Form Spherical Clusters. Angew. Chem. Int. Ed. 2016, 55 (14), 4504–4508. https://doi.org/10.1002/anie.201511857.

(13) Shaikh, H.; Rho, J. Y.; Macdougall, L. J.; Gurnani, P.; Lunn, A. M.; Yang, J.; Huband, S.; Mansfield, E. D. H.; Peltier, R.; Perrier, S. Hydrogel and Organogel Formation by Hierarchical Self-Assembly of Cyclic Peptides Nanotubes. Chem. – Eur. J. 2018, 24 (71), 19066–19074. https://doi.org/10.1002/chem.201804576.

(14) Granja, J. R.; Ghadiri, M. R. Channel-Mediated Transport of Glucose across Lipid Bilayers. J. Am. Chem. Soc. 1994, 116 (23), 10785–10786. https://doi.org/10.1021/ja00102a054.

(15) Ghadiri, M. R.; Granja, J. R.; Buehler, L. K. Artificial Transmembrane Ion Channels from Self-Assembling Peptide Nanotubes. Nature 1994, 369 (6478), 301–304. https://doi.org/10.1038/369301a0.

(16) García-Fandiño, R.; Amorín, M.; Castedo, L.; Granja, J. R. Transmembrane Ion Transport by Self-Assembling α,γ-Peptide Nanotubes. Chem. Sci. 2012, 3 (11), 3280–3285. https://doi.org/10.1039/C2SC21068A.

(17) Montenegro, J.; Ghadiri, M. R.; Granja, J. R. Ion Channel Models Based on Self-Assembling Cyclic Peptide Nanotubes. Acc. Chem. Res. 2013, 46 (12), 2955–2965. https://doi.org/10.1021/ar400061d.

(18) Bakker, M. H.; Kieltyka, R. E.; Albertazzi, L.; Dankers, P. Y. W. Modular Supramolecular Ureidopyrimidinone Polymer Carriers for Intracellular Delivery. RSC Adv. 2016, 6 (112), 110600–110603. https://doi.org/10.1039/C6RA22490C.

(19) Müllner, M.; Yang, K.; Kaur, A.; New, E. J. Aspect-Ratio-Dependent Interaction of Molecular Polymer Brushes and Multicellular Tumour Spheroids. Polym. Chem. 2018, 9 (25), 3461–3465. https://doi.org/10.1039/C8PY00703A.

(20) Foster, J. C.; Varlas, S.; Couturaud, B.; Coe, Z.; O'Reilly, R. K. Getting into Shape: Reflections on a New Generation of Cylindrical Nanostructures' Self-Assembly Using Polymer Building Blocks. J. Am. Chem. Soc. 2019, 141 (7), 2742–2753. https://doi.org/10.1021/jacs.8b08648.

(21) Birault, A.; Molina, E.; Trens, P.; Cot, D.; Toquer, G.; Marcotte, N.; Carcel, C.; Bartlett, J. R.; Gérardin, C.; Man, M. W. C. Periodic Mesoporous Organosilicas from Polyion Complex Micelles – Effect of Organic Bridge on Nanostructure. EurJIC. 2019, 27 (3157–3164). https://doi.org/10.1002/ejic.201900487.

(22) Wijnands, S. P. W.; Meijer, E. W.; Merkx, M. DNA-Functionalized Supramolecular Polymers: Dynamic Multicomponent Assemblies with Emergent Properties. Bioconjug. Chem. 2019, 30 (7), 1905–1914. https://doi.org/10.1021/acs.bioconjchem.9b00095.

(23) Haedler, A. T.; Kreger, K.; Issac, A.; Wittmann, B.; Kivala, M.; Hammer, N.; Köhler, J.; Schmidt, H.-W.; Hildner, R. Long-Range Energy Transport in Single Supramolecular Nanofibres at Room Temperature. Nature 2015, 523 (7559), 196–199. https://doi.org/10.1038/nature14570.

(24) Han, S.; Pensec, S.; Yilmaz, D.; Lorthioir, C.; Jestin, J.; Guigner, J.-M.; Niepceron, F.; Rieger, J.; Stoffelbach, F.; Nicol, E.; Colombani, O.; Bouteiller, L. Straightforward Preparation of Supramolecular Janus Nanorods by Hydrogen Bonding of End-Functionalized Polymers. Nat. Commun. 2020, 11 (1), 4760. https://doi.org/10.1038/s41467-020-18587-2.

(25) Tang, J.; Quinlan, P. J.; Tam, K. C. Stimuli-Responsive Pickering Emulsions: Recent Advances and Potential Applications. Soft Matter 2015, 11 (18), 3512–3529. https://doi.org/10.1039/C5SM00247H.

(26) Boott, C. E.; Gwyther, J.; Harniman, R. L.; Hayward, D. W.; Manners, I. Scalable and Uniform 1D Nanoparticles by Synchronous Polymerization, Crystallization and Self-Assembly. Nat. Chem. 2017, 9 (8), 785–792. https://doi.org/10.1038/nchem.2721.

(27) Petzetakis, N.; Dove, A. P.; O'Reilly, R. K. Cylindrical Micelles from the Living Crystallization-Driven Self-Assembly of Poly(Lactide)-Containing Block Copolymers. 2011, 2, 955–960. https://doi.org/10.1039/C0SC00596G.

(28) Grubbs, R. B.; Sun, Z. Shape-Changing Polymer Assemblies. Chem. Soc. Rev. 2013, 42, 7436–7445. https://doi.org/10.1039/C3CS60079C.

(29) Mai, Y.; Eisenberg, A. Self-Assembly of Block Copolymers. Chem. Soc. Rev. 2012, 41 (18), 5969–5985. https://doi.org/10.1039/C2CS35115C.

(30) Hayward, R. C.; Pochan, D. J. Tailored Assemblies of Block Copolymers in Solution: It Is All about the Process. Macromolecules 2010, 43 (8), 3577–3584. https://doi.org/10.1021/ma9026806.

(31) Fielding, L. A.; Derry, M. J.; Ladmiral, V.; Rosselgong, J.; Rodrigues, A. M.; Ratcliffe, L. P. D.; Sugihara, S.; Armes, S. P. RAFT Dispersion Polymerization in Non-Polar Solvents: Facile Production of Block Copolymer Spheres, Worms and Vesicles in n-Alkanes. Chem. Sci. 2013, 4 (5), 2081–2087. https://doi.org/10.1039/C3SC50305D.

(32) Tian, Q.; Fei, C.; Yin, H.; Feng, Y. Stimuli-Responsive Polymer Wormlike Micelles. Prog. Polym. Sci. 2019, 89, 108–132. https://doi.org/10.1016/j.progpolymsci.2018.10.001.

(33) Israelachvili, J. Part 3. Self-Assembling Structures and Biological Systems. In Intermolecular & Surface Forces; Academic Press: London, 1991.

(34) Nicolai, T.; Colombani, O.; Chassenieux, C. Dynamic Polymeric Micelles versus Frozen Nanoparticles Formed by Block Copolymers. Soft Matter 2010, 6, 3111–3118. https://doi.org/10.1039/B925666K.

(35) Blanazs, A.; Armes, S. P.; Ryan, A. J. Self-Assembled Block Copolymer Aggregates: From Micelles to Vesicles and Their Biological Applications. Macromol. Rapid Commun. 2009, 30 (4–5), 267–277. https://doi.org/10.1002/marc.200800713.

(36) Mellot, G.; Guigner, J.-M.; Jestin, J.; Bouteiller, L.; Stoffelbach, F.; Rieger, J. Bisurea-Functionalized RAFT Agent: A Straightforward and Versatile Tool toward the Preparation of Supramolecular Cylindrical Nanostructures in Water. Macromolecules 2018, 51 (24), 10214–10222. https://doi.org/10.1021/acs.macromol.8b02156.

(37) Mellot, G.; Guigner, J.-M.; Bouteiller, L.; Stoffelbach, F.; Rieger, J. Templated PISA: Driving Polymerization-Induced Self-Assembly towards Fibre Morphology. Angew. Chem. Int. Ed. 2019, 58 (10), 3173–3177. https://onlinelibrary.wiley.com/doi/abs/10.1002/anie.201809370.

(38) Chapman, R.; Danial, M.; Koh, M. L.; Jolliffe, K. A.; Perrier, S. Design and Properties of Functional Nanotubes from the Self-Assembly of Cyclic Peptide Templates. Chem. Soc. Rev. 2012, 41 (18), 6023–6041. https://doi.org/10.1039/C2CS35172B.

(39) Catrouillet, S.; Brendel, J. C.; Larnaudie, S.; Barlow, T.; Jolliffe, K. A.; Perrier, S. Tunable Length of Cyclic Peptide–Polymer Conjugate Self-Assemblies in Water. ACS Macro Lett. 2016, 5 (10), 1119–1123. https://doi.org/10.1021/acsmacrolett.6b00586.

(40) Chapman, R.; Bouten, P. J. M.; Hoogenboom, R.; Jolliffe, K. A.; Perrier, S. Thermoresponsive Cyclic Peptide – Poly(2-Ethyl-2-Oxazoline) Conjugate Nanotubes. Chem. Commun. 2013, 49 (58), 6522–6524. https://doi.org/10.1039/C3CC42327A.

(41) Danial, M.; Tran, C. M.-N.; Jolliffe, K. A.; Perrier, S. Thermal Gating in Lipid Membranes Using Thermoresponsive Cyclic Peptide–Polymer Conjugates. J. Am. Chem. Soc. 2014, 136 (22), 8018–8026. https://doi.org/10.1021/ja5024699.

(42) Hartlieb, M.; Catrouillet, S.; Kuroki, A.; Sanchez-Cano, C.; Peltier, R.; Perrier, S. Stimuli-Responsive Membrane Activity of Cyclic-Peptide–Polymer Conjugates. Chem. Sci. 2019, 10 (21), 5476–5483. https://doi.org/10.1039/C9SC00756C.

(43) Larnaudie, S. C.; Brendel, J. C.; Jolliffe, K. A.; Perrier, S. PH-Responsive, Amphiphilic Core–Shell Supramolecular Polymer Brushes from Cyclic Peptide–Polymer Conjugates. ACS Macro Lett. 2017, 6 (12), 1347–1351. https://doi.org/10.1021/acsmacrolett.7b00728.

(44) Otter, R.; Klinker, K.; Spitzer, D.; Schinnerer, M.; Barz, M.; Besenius, P. Folding Induced Supramolecular Assembly into PH-Responsive Nanorods with a Protein Repellent Shell. Chem. Commun. 2018, 54 (4), 401–404. https://doi.org/10.1039/C7CC08127H.

(45) Otter, R.; Berac, C. M.; Seiffert, S.; Besenius, P. Tuning the Life-Time of Supramolecular Hydrogels Using ROS-Responsive Telechelic Peptide-Polymer Conjugates. Eur. Polym. J. 2019, 110, 90–96. https://doi.org/10.1016/j.eurpolymj.2018.11.019.

(46) Song, Q.; Yang, J.; Hall, S. C. L.; Gurnani, P.; Perrier, S. Pyridyl Disulfide Reaction Chemistry: An Efficient Strategy toward Redox-Responsive Cyclic Peptide–Polymer Conjugates. ACS Macro Lett. 2019, 8 (10), 1347–1352. https://doi.org/10.1021/acsmacrolett.9b00538.

(47) Song, Q.; Yang, J.; Rho, J. Y.; Perrier, S. Supramolecular Switching of the Self-Assembly of Cyclic Peptide–Polymer Conjugates via Host–Guest Chemistry. Chem. Commun. 2019, 55 (36), 5291–5294. https://doi.org/10.1039/C9CC01914F.

(48) Sun, L.; Fan, Z.; Wang, Y.; Huang, Y.; Schmidt, M.; Zhang, M. Tunable Synthesis of Self-Assembled Cyclic Peptide Nanotubes and Nanoparticles. Soft Matter 2015, 11 (19), 3822–3832. https://doi.org/10.1039/C5SM00533G.

(49) Sikder, A.; Ghosh, S. Hydrogen-Bonding Regulated Assembly of Molecular and Macromolecular Amphiphiles. Mater. Chem. Front. 2019, 3, 2602–2607. https://doi.org/10.1039/C9QM00473.

(50) Isare, B.; Pensec, S.; Raynal, M.; Bouteiller, L. Bisurea-Based Supramolecular Polymers: From Structure to Properties Dedicated to Professor Jean-Pierre Vairon on the Occasion of His 78th Birthday. Comptes Rendus Chim. 2016, 19 (1), 148–156. https://doi.org/10.1016/j.crci.2015.06.013.

(51) Canevet, D.; Sallé, M.; Zhang, G.; Zhang, D.; Zhu, D. Tetrathiafulvalene (TTF) Derivatives: Key Building-Blocks for Switchable Processes. Chem. Commun. 2009, No. 17, 2245–2269. https://doi.org/10.1039/B818607N.

(52) Schröder, H. V.; Schalley, C. A. Tetrathiafulvalene – a Redox-Switchable Building Block to Control Motion in Mechanically Interlocked Molecules. Beilstein J. Org. Chem. 2018, 14 (1), 2163–2185. https://doi.org/10.3762/bjoc.14.190.

(53) Choisnet, T.; Canevet, D.; Sallé, M.; Nicol, E.; Niepceron, F.; Jestin, J.; Colombani, O. Robust Supramolecular Nanocylinders of Naphthalene Diimide in Water. Chem. Commun. 2019, 55 (64), 9519–9522. https://doi.org/10.1039/C9CC04723A.

(54) Choisnet, T.; Canevet, D.; Sallé, M.; Lorthioir, C.; Bouteiller, L.; Woisel, P.; Niepceron, F.; Nicol, E.; Colombani, O. Colored Janus Nanocylinders Driven by Supramolecular Coassembly of Donor and Acceptor Building Blocks. ACS Nano 2021, 15 (2), 2569–2577. https://doi.org/10.1021/acsnano.0c07039.

(55) Akutagawa, T.; Kakiuchi, K.; Hasegawa, T.; Noro, S.; Nakamura, T.; Hasegawa, H.; Mashiko, S.; Becher, J. Molecularly Assembled Nanostructures of a Redox-Active Organogelator. Angew. Chem. Int. Ed. 2005, 44 (44), 7283–7287. https://doi.org/10.1002/anie.200502336.

(56) Liu, Y.; Liu, L.; Zhu, E.; Yue, M.; Gao, C.; Wu, X.; Che, G.; Liu, H. Gel Formed by Self-Assembly of a Urea-Modified Monopyrrolotetrathiafulvalene Derivative Displays Multi-Stimuli Responsiveness and Absorption of Rhodamine B. ChemPlusChem 2018, 83 (12), 1109–1118. https://doi.org/10.1002/cplu.201800442.

(57) Liu, Y.; Wang, Y.; Jin, L.; Chen, T.; Yin, B. MPTTF-Containing Tripeptide-Based Organogels: Receptor for 2,4,6-Trinitrophenol and Multiple Stimuli-Responsive Properties. Soft Matter 2016, 12 (3), 934–945. https://doi.org/10.1039/C5SM02462E.

(58) Wang, C.; Zhang, D.; Zhu, D. A Low-Molecular-Mass Gelator with an Electroactive Tetrathiafulvalene Group: Tuning the Gel Formation by Charge-Transfer Interaction and Oxidation. J. Am. Chem. Soc. 2005, 127 (47), 16372–16373. https://doi.org/10.1021/ja055800u.

(59) Bigot, J.; Charleux, B.; Cooke, G.; Delattre, F.; Fournier, D.; Lyskawa, J.; Sambe, L.; Stoffelbach, F.; Woisel, P. Tetrathiafulvalene End-Functionalized Poly(N-Isopropylacrylamide): A New Class of Amphiphilic Polymer for the Creation of Multistimuli Responsive Micelles. J. Am. Chem. Soc. 2010, 132 (31), 10796–10801. https://doi.org/10.1021/ja1027452.

(60) Sambe, L.; Belal, K.; Stoffelbach, F.; Lyskawa, J.; Delattre, F.; Bria, M.; Sauvage, F. X.; Sliwa, M.; Humblot, V.; Charleux, B.; Cooke, G.; Woisel, P. Multi-Stimuli Responsive Supramolecular Diblock Copolymers. Polym Chem 2014, 5 (3), 1031–1036. https://doi.org/10.1039/C3PY01093G.

(61) Jia, C.; Zhang, D.; Xu, W.; Zhu, D. A New Approach to 4-Alkylthio-1,3-Dithiole-2-Thione: An Unusual Reaction of a Zinc Complex of 1,3-Dithole-2-Thione-4,5-Dithiolate. Org. Lett. 2001, 3 (12), 1941–1944. https://doi.org/10.1021/ol015990n.

(62) Pinault, T.; Cannizzo, C.; Andrioletti, B.; Ducouret, G.; Lequeux, F.; Bouteiller, L. Anions as Efficient Chain Stoppers for Hydrogen-Bonded Supramolecular Polymers. Langmuir 2009, 25 (15), 8404–8407. https://doi.org/10.1021/la804138u.

(63) Tian, J.; Ding, Y.-D.; Zhou, T.-Y.; Zhang, K.-D.; Zhao, X.; Wang, H.; Zhang, D.-W.; Liu, Y.; Li, Z.-T. Self-Assembly of Three-Dimensional Supramolecular Polymers through Cooperative Tetrathiafulvalene Radical Cation Dimerization. Chem Eur J 2014, 20 (2), 575–584. https://doi.org/10.1002/chem.201302951.

(64) Adeel, S. M.; Li, Q.; Nafady, A.; Zhao, C.; Siriwardana, A. I.; Bond, A. M.; Martin, L. L. A Systematic Study of the Variation of Tetrathiafulvalene (TTF), $TTF^{+\cdot}$ and TTF^{2+} Reaction Pathways with Water in the Presence and Absence of Light. RSC Adv. 2014, 4 (91), 49789–49795. https://doi.org/10.1039/C4RA08038F.

(65) Wang, Y.; Frasconi, M.; Stoddart, J. F. Introducing Stable Radicals into Molecular Machines. ACS Cent. Sci. 2017, 3 (9), 927–935. https://doi.org/10.1021/acscentsci.7b00219.

(66) Zhang, D.-W.; Tian, J.; Chen, L.; Zhang, L.; Li, Z.-T. Dimerization of Conjugated Radical Cations: An Emerging Non-Covalent Interaction for Self-Assembly. Chem. – Asian J. 2015, 10 (1), 56–68. https://doi.org/10.1002/asia.201402805.

(67) Hansen, C. M. Hansen Solubility Parameters: A User's Handbook, Second Edition; CRC Press, 2007.

(68) Faour, L.; Adam, C.; Gautier, C.; Goeb, S.; Allain, M.; Levillain, E.; Canevet, D.; Sallé, M. Redox-Controlled Hybridization of Helical Foldamers. Chem. Commun. 2019, 55. https://doi.org/10.1039/C9CC02498K.

(69) Wang, C.; Dyar, S. M.; Cao, D.; Fahrenbach, A. C.; Horwitz, N.; Colvin, M. T.; Carmieli, R.; Stern, C. L.; Dey, S. K.; Wasielewski, M. R.; Stoddart, J. F. Tetrathiafulvalene Hetero Radical Cation Dimerization in a Redox-Active [2]Catenane. J. Am. Chem. Soc. 2012, 134 (46), 19136–19145. https://doi.org/10.1021/ja307577t.